Inorganic Chemistry

Article

pubs.acs.org/IC

Zirconium(IV) Metallocavitands As Blue-Emitting Materials

Hassan Iden,[†,‡,§] Wenhua Bi,[†] Jean-François Morin,*[,†,‡] and Frédéric-Georges Fontaine*[,†,§]

[†]Département de Chimie, Université Laval, 1045 Avenue de la Médecine, Québec (Québec), Canada, G1V 0A6

[‡]Centre de Recherche sur les Matériaux Avancés (CERMA), Université Laval, 1045 Avenue de la Médecine, Québec (Québec), Canada, G1V 0A6

[§]Centre de Catalyse et Chimie Verte (C3 V), Université Laval, 1045 Avenue de la Médecine, Québec (Québec), Canada, G1V 0A6

Supporting Information

ABSTRACT: A series of zirconium-carboxylate metallocavitands with the general formula $[(CpZr)_3(\mu\text{-}\kappa_2,O',O''CR)_3(\mu_3\text{-}O)(\mu_2\text{-}OH)_3]Cl$ (Cp = cyclopentadienyl; R = C_5H_4N (**5**), C_6H_7N (**6**), $C_{18}H_{14}N$ (**7**), and $C_{18}H_{12}N$ (**8**)) were synthesized in moderate to high yields (40−83%) by reacting the corresponding carboxylic acids **1**−**4** with Cp_2ZrCl_2 in a self-assembly procedure at room temperature. The metallocavitands were characterized using ^1H and ^{13}C NMR spectroscopy and by single-crystal X-ray diffraction. Complexes **7** and **8** exhibit efficient photoluminescence properties in solution. The photoluminescence peak of **7** was observed at 464 nm and that of **8** at 422 nm with respective quantum yields in solution of 87 and 65%.

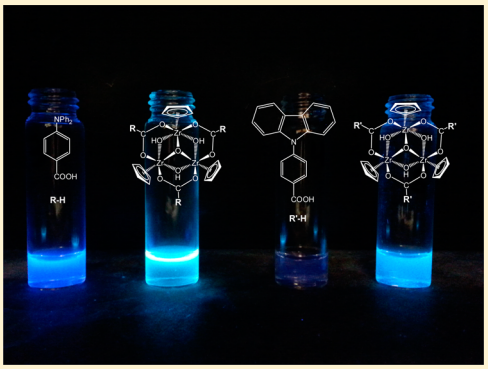

INTRODUCTION

Host−guest systems are at the core of molecular recognition and supramolecular catalysis.[1] Most of the systems reported to date are based on well-known and studied organic cavitands[2] such as calixarenes,[3] cucurbiturils,[4] cyclotriveratrylenes,[5] cyclodextrins,[6] resorci-*n*-arenes,[7] and their derivatives. Their intrinsic cavities have generated a lot of interest since they can encapsulate small molecules through noncovalent interactions and can be used as functional materials for separation,[5a,8] catalysis,[9] molecular sensing,[10] and fullerene encapsulation.[5a,8a,11]

Although tailoring of the cavitands for the desired applications is possible, the synthetic procedures to do so can be tedious and often require multistep syntheses. An interesting alternative to the synthesis of organic cavitands is the self-assembly between organic ligands and inorganic cores generating metallocavitands, a subclass of cavitands.[12] The metallocavitands possess many advantages over their traditional organic analogues. First, the size and the shape of their cavities can be easily controlled by changing the nature of the metal center and of the organic ligands. By adopting ligands having specific geometries and symmetries, and by controlling the coordination sites around the metal interacting with these ligands, novel architectures can be achieved. Second, special properties can be expected for the metallocavitands arising from the presence of metal centers, which can offer potential applications in various fields, such as in chemical sensing and catalysis.[12] Last but not least, a major advantage of metallocavitands lies in their synthetic simplicity because of the high efficiency of the self-assembly process. Furthermore, the large accessibility of organic ligands can lead to the generation of complex structures with an unrestricted number of geometries, allowing the synthesis of a wide variety of cavitands with specific chemical functions.

Recently, we reported a series of trinuclear tantalum boronate half-sandwich metallocavitands where the center of the cavity is composed of an aggregated trimetallic tantalum(V) cluster stabilized by oxo and μ-O_2BR bridges.[13] These species can be easily generated from arylboronic acids and Cp^*TaMe_4 (Scheme 1). The metallocavitands have been shown to interact specifically with Lewis bases such as acetone and tetrahydrofuran by an interaction between the nucleophilic part of the organic molecules and the electrophilic metallic core. Pursuing our work on metallocavitands, we investigated the synthesis of zirconium carboxylate species that would have a similar C_3 symmetry, but without the electrophilic cavity, by the replacement of the boron and tantalum atoms by carbon and zirconium atoms, respectively. Indeed, we expected for these species to show better stability since the B−R bond has been shown to exhibit cleavage in some conditions.[13b]

Zirconium is one of the cheapest transition metals, and its coordination chemistry is well established. While the self-assembly of zirconium clusters in the presence of organic ligands in water has attracted less attention from chemists, probably due to the high reactivity and low stability of zirconium precursors in the presence of moisture or oxygen, some precedents exist demonstrating the ability of zirconium species to generate polymetallic clusters that could lead to the synthesis of metallocavitands.[14] For instance, the hydrolysis of

Received: October 15, 2013
Published: February 26, 2014

   dx.doi.org/10.1021/ic402602d | *Inorg. Chem.* 2014, 53, 2883−2891

Scheme 1. Typical Synthesis of Tantalum Boronate Metallocavitands (R = Aryl Group; the Hydroxyl Groups Were Omitted in the Structure)

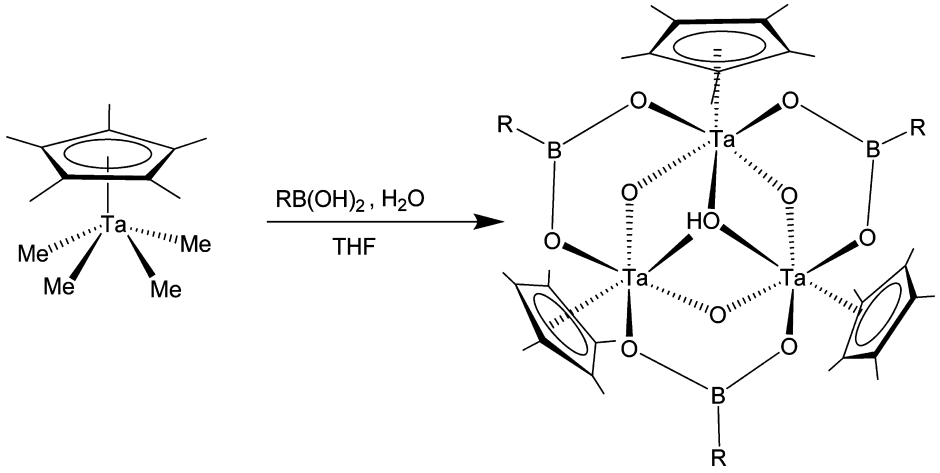

$[(\eta^5\text{-}C_5Me_5)ZrCl_3]$ with a stoichiometric amount of water in toluene at 80 °C yields the trinuclear complex $[\{(\eta^5\text{-}C_5Me_5)ZrCl\}_3(\mu\text{-}Cl)_4(\mu_3\text{-}O)]$ (**A**) with C_s symmetry (Figure 1A),[15] and the hydrolysis of $[Cp_2ZrCH_3(THF)]BPh_4$, "Jordan's cation," in a mixture of dichloromethane/THF at −78 °C yields similar trinuclear $[(Cp_2Zr)_3(\mu_2\text{-}OH)_3(\mu_3\text{-}O)]BPh_4$ complex (**B**) with C_{3V} symmetry (Figure 1B).[16] As described above, in order to get isoelectronic structures to the tantalum boronate species, the ligands of choice for zirconium are the arylcarboxylates. Some zirconium(IV) arylcarboxylate derivatives have been prepared through the reaction of the carboxylate salts with Cp_2ZrCl_2.[17] Indeed, half-sandwich metallocavitands such as $[(CpZr)_3(\mu_3\text{-}O)(\mu_2\text{-}OH)_3(\mu_2\text{-}O',O''C\text{-}C_6HF_4)_3]^+\cdot(C_6HF_4CO_2^-)$ (**C**; Figure 1C),[18] $[(CpZr)_3(\mu_2\text{-}O',O''C\text{-}C_6H_3Cl_2)_3(\mu_3\text{-}OH)(\mu_2\text{-}OH)_3]\text{-}(Cl_2C_6H_3CO_2^-)_2$ (**D**; Figure 1D), and $[(CpZr)_3(\mu_2\text{-}O',O''C\text{-}C_6H_4Cl)_3(\mu_3\text{-}OH)(\mu_2\text{-}OH)_3]Cl_2\cdot CH_2Cl_2$ (**E**; Figure 1E)[19] have been synthesized using a self-assembly approach in aqueous media. To the best of our knowledge, two general synthetic procedures were reported so far, either from a sodium ethoxide mediated assembly of carboxylic acids with Cp_2ZrCl_2 (**C**) or by the assembly of carboxylic acids and Cp_2ZrCl_2 in aqueous dichloromethane (Figure 1D and E).

In order to further expand the properties of zirconium metallocavitands as possible hosts for sensing applications, we investigated the synthesis of zirconium analogues containing extended cavities with nitrogen-containing carboxylate ligands. It was our interest to determine if the presence of functional groups on the organic moieties would impede the formation of the expected metallocavitands, since all half-sandwich metallocavitands reported to date only have aryl groups containing strong C−X bonds.[15−19] Also, several nitrogen-containing aromatic molecules, notably containing the carbazole and the diphenylamine moieties, exhibit interesting photoluminescence properties that could serve as spectroscopic probes for the characterization of host−guest interactions.[20] We herein report the synthesis and characterization of four new half-sandwich metallocavitands having amino, diphenylamino, carbazolyl, and pyridyl moieties. It is possible to demonstrate that the presence of the metallic core has a positive influence on the blue luminescence of the conjugated carboxylate ligands.

RESULTS AND DISCUSSION

Synthesis of Zirconium(IV) Metallocavitands. Following the procedure depicted in Scheme 2, compounds **5**−**8** of general structure $[(CpZr)_3(\kappa_2,O',O''CR)_3(\mu_3\text{-}O)(\mu_2\text{-}OH)_3]\cdot HCl$ (where R = C_5H_4N (**5**), *para*-C_6H_4−NH_2 (**6**), *para*-C_6H_4−$N(C_6H_5)_2$ (**7**), and *para*-C_6H_4−$N(C_{12}H_8)$ (**8**)) were prepared in moderate to good yields (40−83%) by reacting the corresponding carboxylic acids **1**−**4** with a 1 M solution of Cp_2ZrCl_2 in a 2:1 solution of dichloromethane in water at pH 7. Whereas the isonicotic acid and the 4-aminobenzoic acid needed in order to generate species **5** and **6**, respectively, are commercially available, carboxylic acids **3** and **4** were prepared using a cross-coupling methodology (Scheme 3). The key intermediates to synthesize the former carboxylic acids, ethyl 4-(diphenylamino)benzoate and ethyl 4-(9*H*-carbazol-9-yl) benzoate, were prepared via an Ullman-type reaction where 4-iodoethylbenzoate was coupled to diphenylamine and carbazole to afford the esters in 87 and 75% yield, respectively. Hydrolysis of the esters in a mixture of 9:1 $EtOH/H_2O$ at 60 °C afforded the desired carboxylic acids **3** and **4** in 83 and 80% yield, respectively.

The coordination of the carboxylate moiety on the zirconium cluster was monitored using ^1H NMR spectroscopy. The cyclopentadienyl resonances appeared at δ = 6.72, 6.50, 6.81, and 7.03 for complexes **5**−**8**, respectively, which represented significant downfield shifts in comparison to the resonance for Cp_2ZrCl_2 (6.31 ppm). The μ_3-OH was only observed for complex **6** in polar aprotic solvents at 9.80 ppm; it was also possible to observe the presence of the carboxylate ligands in all complexes in a 1:1 ratio to the cyclopentadienyl rings. Moreover, the ^{13}C NMR spectra of all complexes did show a significant downfield shift for all carbon resonances compared to the free ligands, a consequence of the electronic transfer from the ligand to the metal center.

Structural Study of the Metallocavitands. Colorless crystals suitable for X-ray diffraction studies were obtained at room temperature from a solution of methanol for **5**, ether for **7**, and acetone for **8**. All the crystals are air-stable, and the ORTEP representations are presented in Figures 2−4. According to their X-ray structures, the central core of all molecules is composed of a Zr_3O_{10} cluster with pseudo-C_{3v} symmetry. These zirconium centers are in a slightly distorted octahedral environment with the cyclopentadienyl ligand *trans*

dx.doi.org/10.1021/ic402602d | Inorg. Chem. 2014, 53, 2883−2891

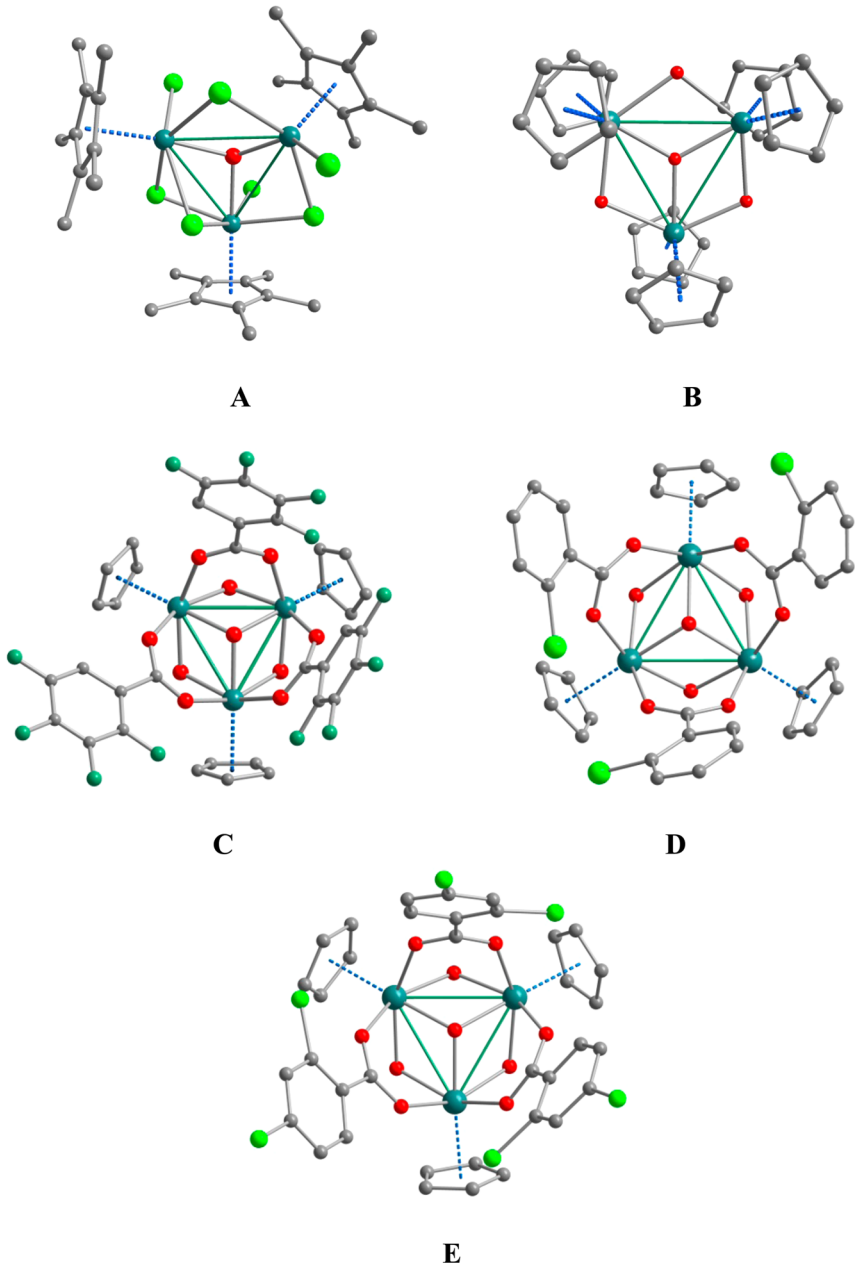

Figure 1. Solid state structures of $[\{(\eta^5\text{-}C_5Me_5)ZrCl\}_3(\mu\text{-}Cl)_4(\mu_3\text{-}O)]$ (**A**),[15] $[(Cp_2Zr)_3(\mu_2\text{-}OH)_3(\mu_3\text{-}O)^+]$ (**B**),[16] $([(CpZr)_3(\mu_3\text{-}O)(\mu_2\text{-}OH)_3(C_6HF_4CO_2)_3]^+\cdot(C_6HF_4CO_2^-))$ (**C**),[18] $[(CpZr)_3(\mu_2\text{-}O',O''C\text{-}C_6H_3Cl_2)_3(\mu_3\text{-}OH)(\mu_2\text{-}OH)_3](Cl_2C_6H_3COO)_2$ (**D**),[19] and $[(CpZr)_3(\mu_2\text{-}O',O''C\text{-}C_6H_4Cl)_3(\mu_3\text{-}OH)(\mu_2\text{-}OH)_3]Cl_2\cdot CH_2Cl_2$ (**E**).[19] Carbon in gray; chlorine in green; oxygen in red; zirconium in cyan.

to the μ_3-O and the bridging carboxylate *cis* to the μ_2-hydroxyl groups (see Figure 5 for a model of the metallic cluster). Due to the steric bulk of the cyclopentadienyl ligand, the octahedrons are heavily distorted, and the four equatorial O atoms are greatly pushed toward the apex of μ_3-O. The μ_3-O atom and the three μ_2-OH's form a slightly distorted tetrahedron with three of the four triangular faces capped with the Zr atoms. A model of the tetrahedron and of the octahedrons is represented in Figure 6.

In the crystal structure of **5**, the pyridinyl groups are protonated as can be deduced by the presence of four chloride anions that are linked by hydrogen bonds (see Figure S20, SI). In the packing of compound **5**, every two adjacent cationic complexes are combined tightly by strong $\pi-\pi$ interactions between the cyclopentadienyl planes (distance of 3.560 Å) to form molecular pairs, as shown in Figure 7. The neighboring pairs are further linked together by hydrogen bonds between the chlorides and the μ_2-OH groups and the methanol molecule present in the crystal lattice to form double-layered sheets in the $b-c$ plane (see Figure S19, SI). The sheets are packed together along the a axis to form the final structure. Water molecules are also present in the structure but are heavily disordered.

The organic groups in **7** are much more flexible than those in **5** due to the presence of the phenyl rings on the nitrogen atoms. The free rotation of the phenyl groups partially blocks the cavity of the metallocavitand. Although two ether molecules are present in the structure, none of them are located within the cavity. The μ_2-OH groups form strong hydrogen bonds with the Cl^- (O3−Cl1 = 3.017(3) Å, O3−H3O−Cl1 = 154.0(2)°)

dx.doi.org/10.1021/ic402602d | *Inorg. Chem.* 2014, 53, 2883−2891

Scheme 2. Synthesis of Zirconium(IV) Metallocavitands by a Self-Assembly Process from Cp_2ZrCl_2

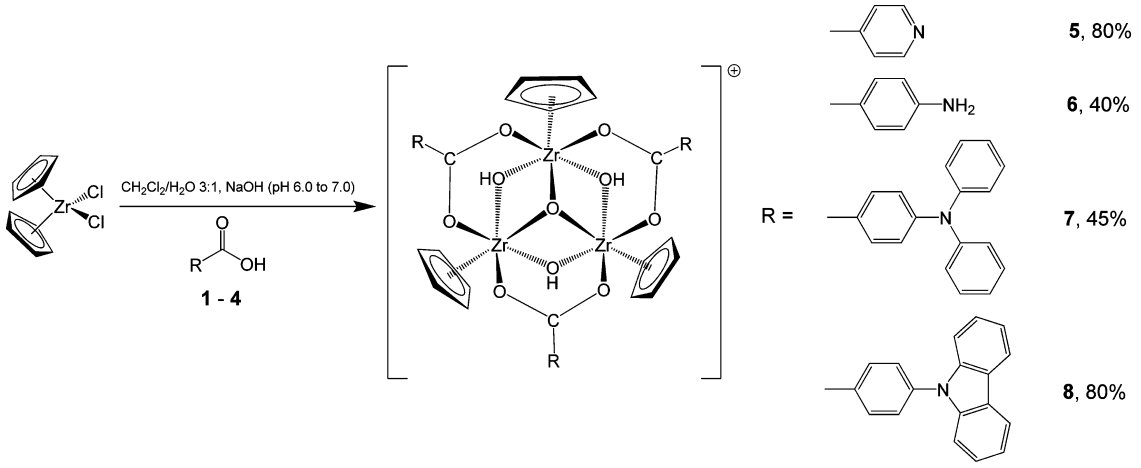

Scheme 3. Synthesis of the Carboxylic Acids 3 and 4 (NR_2 = NPh_2 and Carbazol-9-yl, Respectively)

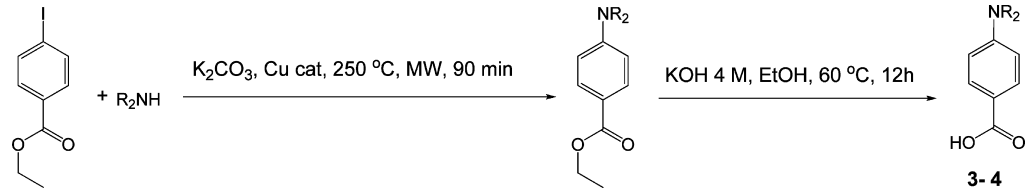

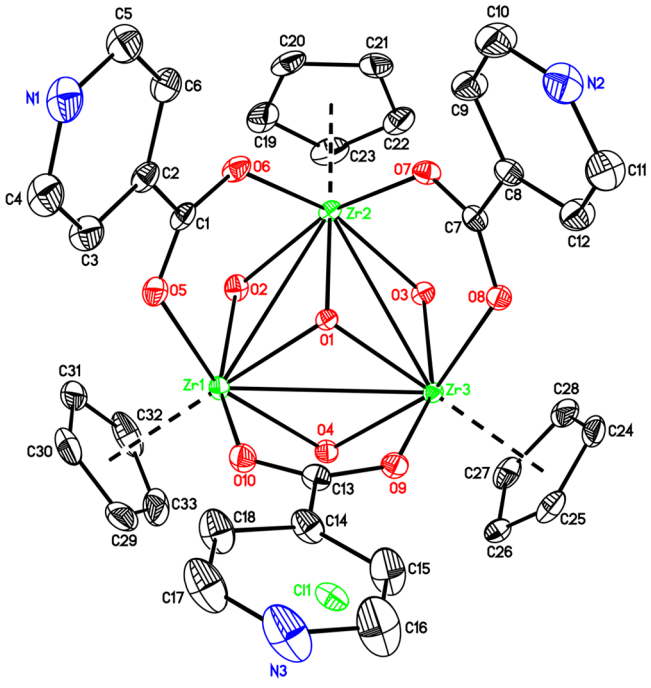

Figure 2. The ORTEP plot of **5** with 50% probability. All hydrogen atoms and solvent molecules are omitted for clarity.

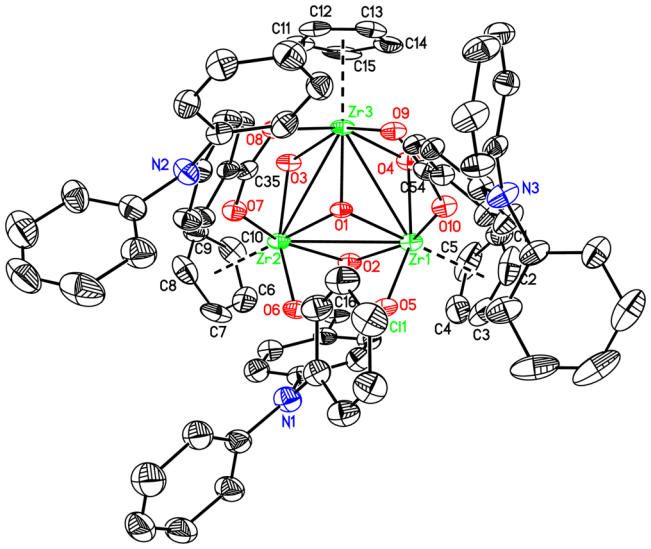

Figure 3. The ORTEP plot of **7** with 50% probability. All hydrogen atoms and solvent molecules are omitted for clarity.

and with the oxygen atom of one of the ether molecules (O4–O11 = 2.950(5) Å, O4–H4O–O11 = 144.30(2)°). The complexes in the crystal structure of **5** are assembled together to form single layers in the *a*–*c* plane, with the different layers further packed together along the *b* axis to form a 3D structure. One more ether molecule is located between the spacing of adjacent cations, as illustrated in Figure S21 (see SI).

Although the carbazole ring is more rigid than the diphenylamine moiety, it is possible to observe that the large heteroaromatic fragment can rotate easily along the N–C single bond in the crystal structure of **8**. One consequence of this behavior is the presence of two crystallographic independent $[(CpZr)_3(\kappa_2,O',O''CR)_3(\mu_3\text{-}O)(\mu_2\text{-}OH)_3]^+$ (R = carbazole) cations in the asymmetric unit. Even if there is rotation between the plane of the phenyl groups and of the carbazole moiety, the cavity is wide enough to have one acetone molecule captured in one of the independent molecules of **8**, while there is no guest molecule in the second cavity (see Figure S23, SI). Five different solvent molecules are located in the structure, two of them with occupancy factors of 0.8 and 0.5, respectively. According to the differential Fourier map, more acetone molecules can be assigned in the structure, but they are heavily

dx.doi.org/10.1021/ic402602d | Inorg. Chem. 2014, 53, 2883–2891

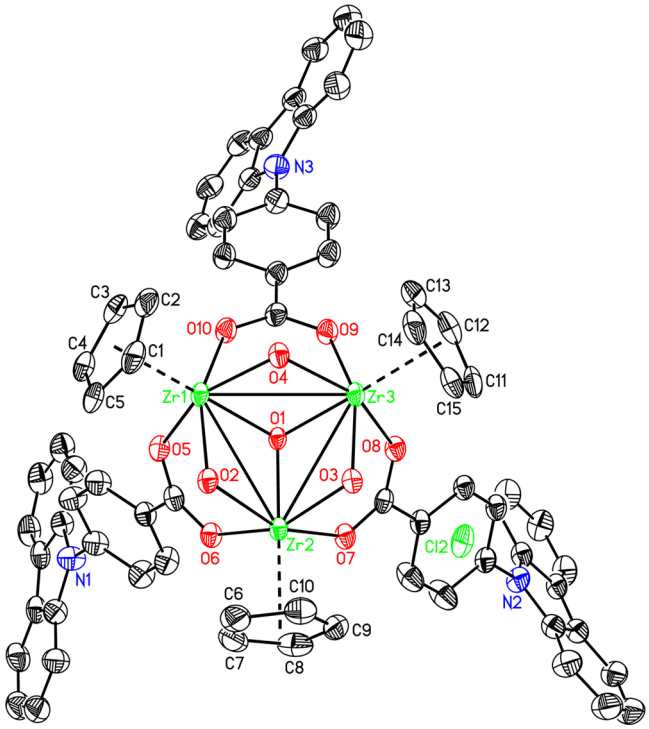

Figure 4. The ORTEP plot of **8** with 50% probability. All hydrogen atoms and solvent molecules are omitted for clarity.

disordered over different positions. Strong hydrogen bonds between the μ^2-OH group, the chlorides, and the O atoms of the acetone molecules are found in the structure. Interestingly, two of the first crystallographic independent $[Zr_3O_4H_3Cp_3(RCOO)_3]^+$ cations are combined together in a mouth-to-mouth mode to form a cage where two guest molecules of acetone are sealed. The cages are tightly packed together to form a layer in the $a-b$ plane. As for the second crystallographic independent $[(CpZr)_3(\kappa_2,O',O''CR)_3(\mu_3\text{-}O)(\mu_2\text{-}OH)_3]^+$ species, the cations are interpenetrated into each other in mouth-to-tail mode to form pairs without a guest molecule. These pairs are arranged into layers parallel to the

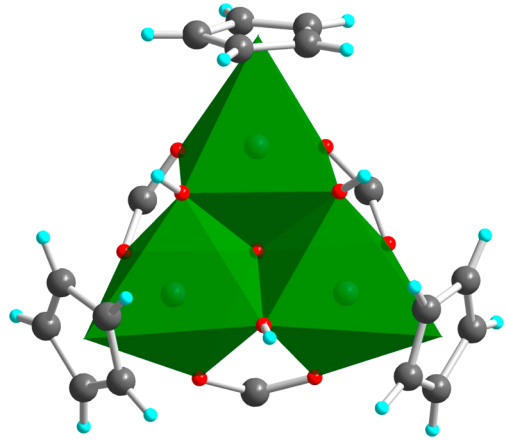

Figure 6. Representation of the tetrahedron and of the three octahedrons in the core of **5**–**8**.

former layer in the $a-b$ plane. Two kinds of layers are packed together alternatively along the c axis to form the 3D structure (see Figure S24, SI).

Contrarily to the neutral $[(Cp^*Ta)_3(\mu_3\text{-}OH)(\mu_2\text{-}OH)(\mu_2\text{-}O)_2(\mu_2\text{-}O_2BR)_3]$ core observed for the tantalum species, the zirconium analogues are observed as cationic $[(CpZr)_3(\mu_3\text{-}O)(\mu_2\text{-}OH)_3(\mu_2\text{-}O_2CR)_3]^+$ species where the charge is balanced by the presence of a chloride in the structure. Therefore, the position of the hydroxyl groups differs in the zirconium species since in the latter complexes a μ_3-O moiety is observed, whereas μ_3-OH is present in the tantalum analogues. As such, species **5**–**8** have three bridging hydroxyl groups, as can be deduced from the longer Zr–O and Zr–Zr distances compared to the Ta–O and Ta–Ta distances. The difference between the shortest and the longest Zr–O distances is very small (ΔM-(μ^2-O) and varies from 0.015 to 0.042 Å in complexes **5**–**8**, whereas the variation can be as important as 0.185 Å in the tantalum metallocavitands, as represented for two characteristic species in Table 1, as a consequence of the presence of two μ-O and one μ-OH in the central core rather than three equidistant μ^2-OH's. The average Zr–(μ_3-O)–Zr bond angles at the central oxygen atom in **5**, **7**, and **8** are nearly the same (108°)

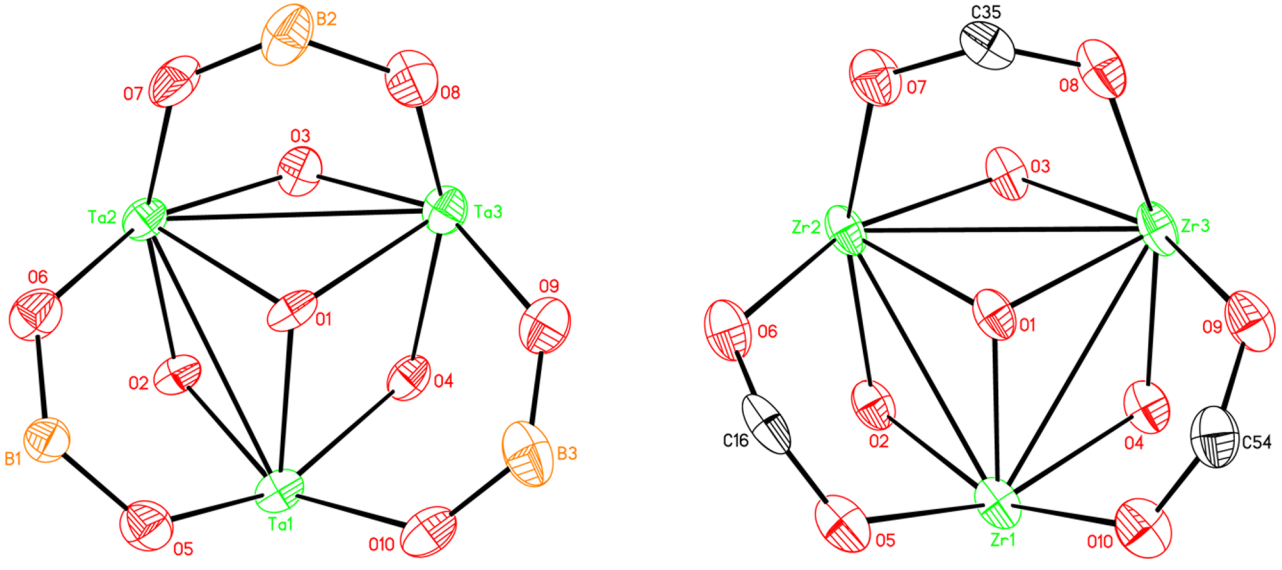

Figure 5. Labeling scheme for the inorganic core in Ta_3O_4 and Zr_3O_4 complexes.

dx.doi.org/10.1021/ic402602d | Inorg. Chem. 2014, 53, 2883–2891

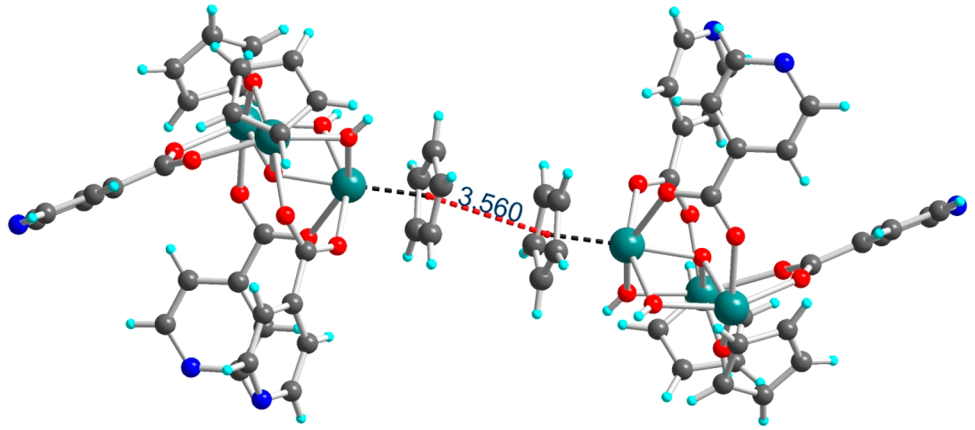

Figure 7. Representation of the strong $\pi-\pi$ interaction between Cp molecules in **5**.

Table 1. Interatomic Distances in the Metallic Core of Zirconium and Tantalum Metallocavitands

complex	dM1−M2 (Å)	dM2−M3 (Å)	dM1−M3 (Å)	av. M-(μ^2-O) (ΔM-(μ^2-O)) (Å)
Ta_3-4OPh[a]	3.322	3.295	3.477	2.02 (0.185)
Ta_3-4PhEt[a]	3.337	3.341	3.407	2.06 (0.080)
Zr_3-4C_5H_5N (**5**)	3.346	3.361	3.341	2.12 (0.015)
Zr_3-4$C_{18}H_{15}N$ (**7**)	3.364	3.354	3.350	2.13 (0.042)
Zr_3-4$C_{18}H_{13}N$ (**8**)	3.361	3.340	3.355	2.12 (0.026)

[a]Values reported in ref 13a.

and are all comparable with those reported for $[(C_5H_5Zr)_3(\mu_3\text{-}O)(\mu_2\text{-}OH)_3(C_6HF_4CO_2)_3]^+\cdot(C_6HF_4CO_2^-)$[18] and $[(CpZr)_3(\mu_2\text{-}O',O''C\text{-}C_6H_3Cl_2)_3(\mu_3\text{-}OH)(\mu_2\text{-}OH)_3]\cdot(Cl_2C_6H_3COO)_2$.[19] Moreover, the metal oxygen distances (Zr−O) observed for all of the carboxylate ligands are longer than those observed for the boronate (B−O) species in the tantalum clusters. This difference can be attributed to the difference in the bonding mode of the carboxylate ligand, which is formally an LX (L = dative, X = covalent) type of bidentate ligand, whereas the boronate is formally an X_2 ligand. The bond distances in the trimetallic cores of **5**, **7**, and **8** are unremarkable compared to the ones in previously reported carboxylate complexes with similar structures (Figure 1 C, D, and E), where the Zr−Zr and Zr−O distances vary from 3.33 to 3.36 Å and 2.10 to 2.14 Å, respectively.[18,19]

As observed in the space-filling representations in Figure 8, all species exhibit the expected C_3 symmetry. In the case of **5**, the presence of the pyridinyl group does not alter significantly the shape of the cavity compared to what was observed in the presence of the phenylboranate tantalum clusters.[13] However, in the case of **7** and **8**, the significant flexibility and the large volume of the diphenylamine and carbazole moieties induce a rotation along the C_{aryl}−N bonds, which blocks in part the cavity. As desired, the modification of the tantalum−boronate core for a zirconium−carboxylate one reduces the electrophilic character of the cavitands since they do not interact with Lewis bases. Indeed, no interaction is observed in solution or in a solid state between the inorganic core and THF or acetone. On the contrary, the species get protonated readily and are observed as $[(CpZr)_3(\mu_3\text{-}O)(\mu_2\text{-}OH)_3(\mu_2\text{-}O_2CR)_3]^+$ cores.

Optical Properties of Metallocavitands. In the past few years, many transition-metal-based organometallic compounds

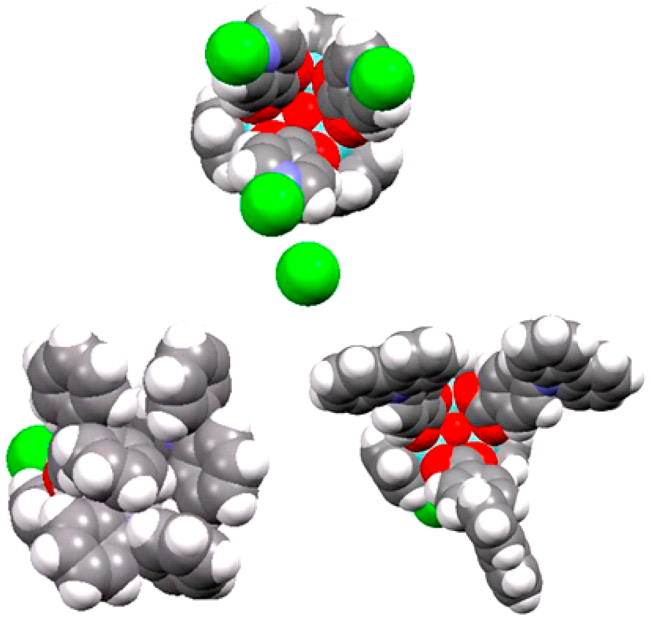

Figure 8. Space-filling views of **5** (top), **7** (down left), and **8** (down right), obtained from crystallographic data. Carbon atoms are in gray; hydrogen atoms are in white; oxygen atoms are in red; zirconium atoms are in navy blue, and nitrogen atoms are in purple.

have attracted attention for their fluorescence and phosphorescence properties in the solid state. When stable under ambient conditions, these compounds become promising candidates for light-emitting diodes.[21] While the red and green region of the visible spectrum can be reached quite easily with organometallic compounds, stable blue emitters with high solid-state quantum yield are much less common due to decomposition[22] or nonradiative deactivation processes.[23] Also, the preparation of blue organometallic emitters requires the use of large $\pi-\pi^*$ energy gap ligands whose electronic properties can be coupled to the metal center through various mechanisms.

The absorption and photoluminescence properties of metallocavitands **7** and **8** have been determined in solution, with the typical spectra in Figure 9, and the results are summarized in Table 2. Both metallocavitands absorb in the UV region and exhibit blue photoluminescence under UV excitation. Interestingly, the absorption and photoluminescence spectra are red-shifted compared to the spectra of their ligands

dx.doi.org/10.1021/ic402602d | Inorg. Chem. 2014, 53, 2883−2891

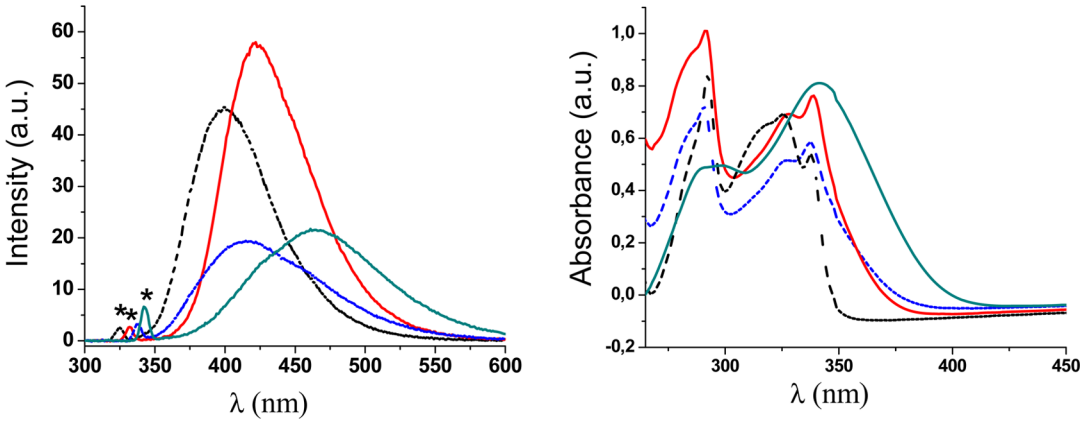

Figure 9. Photoluminescence (left) and absorption (right) spectra of compounds **3** (blue), **4** (black broken line), **7** (dark cyan), and **8** (red solid line). The asterisk (∗) represents the excitation peaks.

Table 2. UV/Vis and Photoluminescence Data for Species Containing the Conjugated Nitrogen Containing Carboxylate Ligands[a]

compound	λ_{max} (absorption) (nm)	λ_{fluo} (nm)	Φ_F[b]	ε (M^{-1} cm^{-1})
3	326	415	0.73	8500
4	327	400	0.66	26 400
7	333	464	0.87	6500
8	342	422	0.65	20 700

[a]All spectra were recorded in THF solutions at room temperature at $c = 1.4 \times 10^{-6}$ to 7.2×10^{-6} M for absorption and photoluminescence. [b]Photoluminescence quantum yields were determined relative to 9,10-diphenylanthracene in cyclohexane ($\Phi_F = 0.9$).

in the carboxylic acid form (**3** and **4**, respectively), suggesting that the effective conjugation length has been increased upon attachment of the ligand to the zirconium center. More experiments need to be performed to assess if these bathochromic shifts are attributed to a donor−acceptor interaction between a nitrogen-containing ligand and the metal center or to the enhanced electro-withdrawing character of the Zr−OOC moieties. The fact that this red-shift is particularly marked in the photoluminescence spectrum of metallocavitand **7**, whose photoluminescence peak is shifted by ca. 50 nm compared to that of ligand **3**, supported this hypothesis since triarylamine is known to be a stronger electron donor than carbazole.[24] Solvatochromism absorption experiments were carried out, and the absorption maxima slightly shift depending on the nature of the solvent. However, since in most solvents, with the exception of THF, there is a presence of partial precipitation and aggregation of the metallocavitands, the interpretation of these data is unreliable.

The photoluminescence quantum yields (Φ_F) of the ligands and their metallocavitands have also been measured using 9,10-diphenylanthracene as the reference. Surprisingly, the Φ_F value increased significantly when the triarylamine was attached to the Zr center (Φ_F = 0.73 and 0.87, for **3** and **7**, respectively), while the Φ_F values are almost identical for **4** and **8**. Moreover, both metallocavitands **7** and **8** are highly fluorescent in the solid state, although Φ_F values could not be measured. These results suggest that these new metallocavitands might be used as efficient blue emitters in light-emitting diodes to enhance the photoluminescence of already efficient carboxylate species.

CONCLUSION

In the present study, the synthesis and characterization of new trinuclear Zr(IV) metallocavitands based on nitrogen-containing carboxylic acids are reported and structurally compared to previously reported Ta(V) boronate metallocavitands. As expected, the inorganic core is more nucleophilic as observed by the protonation of one of the bridging oxygens to generate $[(CpZr)_3(\kappa_2,O',O''CR)_3(\mu_3\text{-}O)(\mu_2\text{-}OH)_3]Cl$ species rather than neutral compounds as observed with tantalum. The possibility of free rotation between the phenyl ring and the diphenylamine and carbazolyl moieties in species **7** and **8**, respectively, induce the blockage of the cavities in the latter complexes. As such, these species does not exhibit significant interactions with the fullerenes.

Nevertheless, these inorganic species are revealed to be excellent blue-emitting materials. The inorganic carboxylate materials are exhibiting a bathochromic shift compared to the corresponding carboxylic acids. Interestingly, the quantum yield of photoluminescence of the diphenylaminobenzoate moiety is significantly enhanced when coordinated on zirconium.

EXPERIMENTAL SECTION

General Procedure. All solvents (ACS grade) were distilled and put through a Vacuum Atmosphere Company (CA, USA) solvent purification system. All of the reagents were purchased from Sigma-Aldrich Co., TCI America, or Oakwood Products and used as received. All reactions were carried out under an atmosphere of argon with freshly distilled solvents, unless otherwise noted. Microwave heating was performed in the single-mode microwave cavity of a Monowave 300 (Anton Paar Co.), and all microwave-irradiated reactions were conducted in heavy-walled glass vials sealed with Teflon septa. Silica gel (SiliaFlash P-60) was used for column chromatography. NMR spectra were recorded on an Agilent Technologies NMR spectrometer at 500 MHz (^{1}H) and 125.758 MHz (^{13}C) or a Varian Inova NMR AS400 spectrometer, at 400.0 MHz (^{1}H) and 100.580 MHz (^{13}C). ^{1}H NMR and ^{13}C NMR chemical shifts are referenced to residual protons or carbons in deuterated solvent. Mass spectra were performed by the Mass Spectrometry Facilities at Laval University with an Agilent 6210 Time-of-Flight (TOF) LC-MS apparatus equipped with an ESI or APPI ion source (Agilent Technologies, Toronto, Canada). UV−vis spectra were measured on a Varian Cary 500 Scan spectrophotometer. The photoluminescence spectra were collected on a Varian Cary Eclipse Spectrofluorometer with excitation and emission slits of 5 nm. All samples were degassed by bubbling nitrogen or argon through the solutions.

Synthesis. *Ethyl 4-(Diphenylamino)benzoate.* Diphenylamine (0.66 g, 4.0 mmol), 4-iodoethyl benzoate (2.0 g, 7.2 mmol), copper

dx.doi.org/10.1021/ic402602d | Inorg. Chem. 2014, 53, 2883−2891

powder (25 mg, 0.4 mmol), and potassium carbonate (1.66 g, 12 mmol) were mixed and stirred at 250 °C for 90 min using microwave irradiation under a nitrogen atmosphere. After the reaction, the reaction mixture was poured into brine, washed, and extracted using dichloromethane. The organic extracts were dried over $MgSO_4$ and concentrated by rotary evaporation. The solid residue was purified by column chromatography (DCM/*n*-hexane = 4:6) and gave the desired product as an off-white solid (1.10 g, 3.5 mmol, 87%). ^{1}H NMR (500 MHz, $CDCl_3$): δ 7.86 (d, J = 7.3 Hz, 2H), 7.30 (t, J = 7.1 Hz, 4H), 7.12 (m, 6H), 6.99 (m, 2H), 4.37−4.30 (q, J = 7.0 Hz, 2H), 1.36 (t, 4.1 Hz, 3H). ^{13}C{^{1}H} NMR (125 MHz, $CDCl_3$): δ 166.4, 151.9, 146.7, 130.8, 129.5, 125.7, 124.3, 122.6, 120.1, 60.5, 14.4. HRMS (ESI): m/z $[M + H]^+$ calcd for $C_{21}H_{20}NO_2$: 318.1485. Found: 318.1489.

Ethyl 4-(9H-Carbazol-9-yl)benzoate. Carbazole (0.66 g, 4.0 mmol), 4-iodoethyl benzoate (2 g, 7.2 mmol), copper powder (25 mg, 0.4 mmol), and potassium carbonate (1.656 g, 12 mmol) were mixed and stirred at 250 °C for 90 min using microwave irradiation under a nitrogen atmosphere. After the reaction was finished, the reaction mixture was poured into brine, washed, and extracted using dichloromethane. The organic extracts were dried over $MgSO_4$ and concentrated by rotary evaporation. The solid residue was purified by column chromatography (DCM/*n*-hexane = 3:7) to give the expected product as an off-white solid (0.95 g, 3.0 mmol, 75%). ^{1}H NMR (500 MHz, $CDCl_3$): δ 8.33−8.28 (m, 2H), 8.19−8.13 (m, 2H), 7.71−7.66 (m, 2H), 7.51−7.40 (m, 4H), 7.36−7.29 (m, 2H), 4.47 (q, J = 7.1 Hz, 2H), 1.47 (t, J = 7.1 Hz, 3H). ^{13}C{^{1}H} NMR (125 MHz, $CDCl_3$): δ 165.9, 141.2, 140.2, 131.3, 129.0, 126.4, 126.2, 123.7, 120.5, 120.4, 109.7, 61.2, 14.4. HRMS (ESI): m/z $[M]^{*+}$ calcd for $C_{21}H_{17}NO_2$: 315.1254. Found: 315.1249.

*4-(Diphenylamino)benzoic acid (**3**).* A solution of ethyl 4-(diphenylamino)benzoate (0.16 g, 0.97 mmol) was dissolved in ethanol (20 mL) and treated with a solution of KOH (20 mL, 4 M), then heated to 60 °C for 12 h. After the completion of the reaction, the solvent was removed in a vacuum and followed by the addition of HCl (1 M solution in water) until it reached a pH ∼ 2. The aqueous solution was extracted with EtOAc (3 × 10 mL), and the organic layers were combined and dried over $MgSO_4$. The solution was filtered and concentrated under reduced pressure to afford the desired acid **3** as a white solid (0.61 g, 83%).^{1}H NMR (500 MHz, $CDCl_3$): δ 7.91 (d, J = 7.9 Hz, 2H), 7.31 (t, J = 7.4 Hz, 4H), 7.14 (m, 6H), 6.98 (m, 2H). ^{13}C{^{1}H} NMR (125 MHz, $CDCl_3$): δ 172.1, 152.7, 146.5, 131.6, 129.6, 126.0, 124.7 121.0, 119.5. HRMS (ESI): m/z $[M + H]^+$ calcd for $C_{19}H_{15}NO_2$: 289.1097. Found: 289.1118.

*4-(9H-Carbazol-9-yl)benzoic Acid (**4**).* A solution of ethyl 4-(9H-carbazol-9-yl)benzoate (0.16 g, 0.97 mmol) was dissolved in ethanol (20 mL) and treated with a solution of KOH (20 mL, 4 M), then heated to 60 °C for 12 h. After the completion of the reaction, the solvent was removed in a vacuum, followed by the addition of HCl (1 M solution in water) until it reached a pH ∼ 2. The aqueous solution was extracted with EtOAc (3 × 10 mL), and the organic layers were combined and dried over $MgSO_4$. The solution was filtered and concentrated under reduced pressure to afford the desired acid **4** (0.61 g, 85%) as a white solid. ^{1}H NMR (500 MHz, $CDCl_3$): δ 8.39 (d, J = 8.5 Hz, 2H), 8.16 (d, J = 7.7 Hz, 2H), 7.76 (d, J = 8.5 Hz, 2H), 7.55−7.50 (m, 2H), 7.48−7.42 (m, 2H), 7.34 (m, 2H). ^{13}C{^{1}H} NMR (125 MHz, $CDCl_3$): δ 171.1, 142.9, 140.1, 132.1, 127.6, 126.4, 126.2, 123.9, 120.7, 120.5, 109.8. HRMS (ESI): m/z $[M]^{*+}$ calcd for $C_{19}H_{15}NO_2$: 287.0941. Found: 287.0961.

Synthesis of Metallocavitands $[(CpZr)_3(\kappa_2,O',O''CR)_3(\mu_3\text{-}O)(\mu_2\text{-}OH)_3]\cdot HCl$. All the cavitands were synthesized according to the same general procedure. Benzoic acid (1.0 mmol) was dissolved in water (5.0 mL), and sodium hydroxide NaOH (1.0 mmol) was then added, and the solution was adjusted to pH 6−7 by addition of hydrochloric acid, when a precipitate was formed. This suspension was then added via pipet dropwise to a solution of zirconocene (Cp_2ZrCl_2, 1.0 mmol) in dichloromethane (15 mL) under vigorous stirring. The reaction mixture was stirred for 15 more minutes at room temperature, and the two-phase system was allowed to separate. The aqueous phase was extracted with dichloromethane (10 mL), and the organic phases were combined. The latter phase was dried over anhydrous $MgSO_4$ and filtered, and the solvent was removed under reduced pressure. The residue was further dried under vacuum conditions to give the crude product, which was further purified by precipitation or crystallization.

*$[(CpZr)_3(\kappa_2,O',O''C\text{-}C_5H_4N)_3(\mu_3\text{-}O)(\mu_2\text{-}OH)_3]\cdot 4HCl$ (**5**).* Compound **5** was synthesized according to the general method described above and crystallized from methanol (white solid, 80%). ^{1}H NMR (500 MHz, DMSO-d_6): δ 8.73 (d, J = 5.7 Hz, 6H), 8.08 (d, J = 5.9 Hz, 6H), 6.72 (s, 15H). ^{13}CNMR (125 MHz, $CDCl_3$): δ 172.6, 149.0, 143.62, 126.1, 118.4. HRMS m/z $[M + H]^+$ or $[M]^{*+}$ not observed by ESI or TOF.

*$[(CpZr)_3(\kappa_2,O',O''C\text{-}C_6H_7N)_3(\mu_3\text{-}O)(\mu_2\text{-}OH)_3]\cdot HCl$ (**6**).* Compound **6** was synthesized according to the general method described above and purified by trituration from tetrahydrofuran (white solid, 40%). ^{1}H NMR (500 MHz, DMSO-d_6): δ 9.80 (s, 3H), 7.57 (d, J = 8.7 Hz, 6H), 6.50 (s, 15H), 6.48 (d, J = 8.7 Hz, 6H). ^{13}C NMR (125 MHz): 173.5, 154.4, 132.6, 117.5, 115.9, 113.0. HRMS (ESI): m/z $[M]^{*+}$ calcd for $C_{36}H_{36}N_3O_{10}Zr_3$: 939.9536. Found: 940.9560.

*$[(CpZr)_3(\kappa_2,O',O''C\text{-}C_{18}H_{15}N)_3(\mu_3\text{-}O)(\mu_2\text{-}OH)_3]\cdot HCl$ (**7**).* Compound **7** was synthesized according to the general method described above and crystallized from acetone (white solid, 45%). ^{1}H NMR (500 MHz, $CDCl_3$): δ 7.75−7.71 (m, 6H), 7.30−7.26 (m, 12H), 7.12−7.09 (m, 18H), 6.93−6.90 (m, 6H), 6.81 (s, 15H). ^{13}C{^{1}H} NMR (125 MHz, $CDCl_3$): δ 172.8, 152.0, 146.7, 131.5, 129.5, 125.7, 124.3, 120.1, 116.5. HRMS (ESI): m/z $[M]^{*+}$ calcd for $C_{72}H_{60}O_{10}N_3Zr_3$: 1396.1414. Found: 1396.1466.

*$[(CpZr)_3(\kappa_2,O',O''C\text{-}C_{18}H_{13}N)_3(\mu_3\text{-}O)(\mu_2\text{-}OH)_3]\cdot HCl$ (**8**).* Compound **8** was synthesized according to the general method described above and crystallized from acetone (white solid, 80%). ^{1}H NMR (500 MHz, $CDCl_3$): δ 8.27 (d, J = 8.4 Hz, 6H), 8.10 (d, J = 7.6 Hz, 6H), 7.66 (d, J = 8.4 Hz, 6H), 7.40 (d, J = 8.2 Hz, 6H), 7.34−7.29 (m, 6H), 7.28−7.24 (m, 6H), 7.03 (s, 15H). ^{13}C{^{1}H} NMR (125 MHz, $CDCl_3$): δ 172.5, 142.2, 140.1, 132.0, 130.7, 126.3, 126.2, 123.7, 120.5, 120.4, 117.0, 109.7. HRMS (ESI): m/z $[M]^{*+}$ calcd for $C_{72}H_{54}O_{10}N_3Zr_3$: 1390.0945. Found: 1390.0956.

Calculation of Photoluminescence Quantum Yield. Photoluminescence quantum yields were calculated using the standard samples which have a fixed and known photoluminescence quantum yield value, according to the following equation:

$$\Phi_F = \Phi_r(I/I_r) \times (OD_r/OD) \times (\eta^2/\eta_r^2)$$

Subscript r represents the standard samples, Φ represents the photoluminescence quantum yield, η represents the refractive index of the solvent, OD represents the calculated area from photoluminescence spectra in cm^{-1}, and I represents the absorbance intensity.

Procedure.

1. Prepare the sample of compounds **3**, **4**, **7**, and **8** having different absorbances between 0.01 and 0.1 at the excitation wavelength of each compound.
2. Measure the photoluminescence spectrum for the entire emission region with the prepared samples using the specific excitation wavelength of the desired compound.
3. Calculate the area in cm^{-1} from the spectrum.
4. Calculate the photoluminescence quantum yield from the equation mentioned above.

Crystallographic Studies. Single crystals with suitable size of all compounds were mounted on CryoLoops with Paratone-N and optically aligned on a Bruker SMART APEX-II X-ray diffractometer with a 1K CCD detector using a digital camera. Initial intensity measurements were performed using a fine-focused sealed tube, graphite-monochromated, X-ray source (Mo Kα, λ = 0.71073 Å) at 50 kV and 30 mA. The standard APEX-II[25] software package was used for determining the unit cells, generating the data collection strategy, and controlling data collection. SAINT[26] was used for data integration including Lorentz and polarization corrections. Semiempirical absorption corrections were applied using SCALE (SADABS).[27] The structures of all compounds were solved by direct methods and refined by full-matrix least-squares methods with SHELX-97[28] in the SHELXTL6.14 package. As the solvent molecules in some compounds

dx.doi.org/10.1021/ic402602d | Inorg. Chem. 2014, 53, 2883−2891

are highly disordered, the SQUEEZE subroutine of the PLATON[29] software suit was used to remove the scattering contributions from the highly disordered guest molecules. The resulting new HKL files were used to further refine the structures. All of the H atoms (on C atoms) were generated geometrically and refined in riding mode. Crystallographic information for all obtained phases is summarized in Table S1. Atomic coordinates and additional structural information are provided in the cif files of the Supporting Information.

■ ASSOCIATED CONTENT

Ⓢ Supporting Information

NMR spectra of species **1**−**8** and additional crystallographic figures are available. This material is available free of charge via the Internet at http://pubs.acs.org. Crystallographic data have been deposited with CCDC (CCDC No. 966119 for **5**, CCDC No. 966120 for **7**, and CCDC No. 966121 for **8**). These data can be obtained upon request from the Cambridge Crystallographic Data Centre, 12 Union Road, Cambridge CB2 1EZ, UK, e-mail: deposit@ccdc.cam.ac.uk, or via the Internet at www.ccdc.cam.ac.uk.

■ AUTHOR INFORMATION

Corresponding Author

*E-mail: frederic.fontaine@chm.ulaval.ca.

Notes

The authors declare no competing financial interest.

■ ACKNOWLEDGMENTS

We are grateful to FQRNT (Projet de recherche en équipe - Québec) and CFI (Canada), CCVC (Québec), and CQMF (Québec) for financial support. We acknowledge the help of Pierre Audet with the HR-MS experiments.

■ REFERENCES

(1) (a) Lehn, J.-M. *Angew. Chem., Int. Ed. Engl.* **1990**, *29*, 1304−1319. (b) Uhlenheuer, D. A.; Petkau, K.; Brunsveld, L. *Chem. Soc. Rev.* **2010**, *39*, 2817−2826.

(2) (a) Higler, I.; Timmerman, P.; Verboom, W.; Reinhoudt, D. N. *Eur. J. Org. Chem.* **1998**, 2689−2702. (b) Cram, D. J. *Science* **1983**, *219*, 1177−1783.

(3) (a) Redshaw, C. *Coord. Chem. Rev.* **2003**, *244*, 45−70. (b) Matthews, S. E.; Beer, P. D. *Supramol. Chem.* **2005**, *17*, 411−435.

(4) (a) Lee, J. W.; Samal, S.; Selvapalam, N.; Kim, H.-J.; Kim, K. *Acc. Chem. Res.* **2003**, *36*, 621−630. (b) Yi, J.-M.; Zhang, Y.-Q.; Cong, H.; Xue, S.-F.; Tao, Z. *J. Mol. Struct.* **2009**, *933*, 112−117.

(5) (a) Hardie, M. J. *Chem. Soc. Rev.* **2010**, *39*, 516−527. (b) Matsubara, H.; Oguri, S.-y.; Asano, K.; Yamamoto, K. *Chem. Lett.* **1999**, *28*, 431−432.

(6) (a) Liu, Y.; Chen, Y. *Acc. Chem. Res.* **2006**, *39*, 681−691. (b) Hapiot, F.; Tilloy, S.; Monflier, E. *Chem. Rev.* **2006**, *106*, 767−781. (c) Jeon, W. S.; Moon, K.; Park, S. H.; Chun, H.; Ko, Y. H.; Lee, J. Y.; Lee, E. S.; Samal, S.; Selvapalam, N.; Rekharsky, M. V.; Sindelar, V.; Sobransingh, D.; Inoue, Y.; Kaifer, A. E.; Kim, K. *J. Am. Chem. Soc.* **2005**, *127*, 12984−12989.

(7) Azov, V. A.; Beeby, A.; Cacciarini, M.; Cheetham, A. G.; Diederich, F.; Frei, M.; Gimzewski, J. K.; Gramlich, V.; Hecht, B.; Jaun, B.; Latychevskaia, T.; Lieb, A.; Lill, Y.; Marotti, F.; Schlegel, A.; Schlittler, R. R.; Skinner, P. J.; Seiler, P.; Yamakoshi, Y. *Adv. Funct. Mater.* **2006**, *16*, 147−156.

(8) J. Hardie, M. J.; Raston, C. L. *Chem. Commun.* **1999**, 1153−1163.

(9) (a) Hooley, R. J.; Rebek, J., Jr. *Chem. Biol.* **2009**, *16*, 255−264. (b) Pinacho Crisóstomo, F. R.; Lledó, A.; Shenoy, S. R.; Iwasawa, T.; Rebek, J., Jr. *J. Am. Chem. Soc.* **2009**, *131*, 7402−7410. (c) Shenoy, S. R.; Pinacho Crisóstomo, F. R.; Iwasawa, T.; Rebek, J., Jr. *J. Am. Chem. Soc.* **2008**, *130*, 5658−5859.

(10) (a) Melegari, M.; Suman, M.; Pirondini, L.; Moiani, D.; Massera, C.; Ugozzoli, F.; Kalenius, E.; Vainiotalo, P.; Mulatier, J.-C.; Dutasta, J.-P.; Dalcanale, E. *Chem.—Eur. J.* **2008**, *14*, 5772−5779. (b) Ballester, P.; Sarmentero, M. A. *Org. Lett.* **2006**, *8*, 3477−3480. (c) Pinalli, R.; Suman, M.; Dalcanale, E. *Eur. J. Org. Chem.* **2004**, 451−462. (d) Pinalli, R.; Dalcanale, E. *Acc. Chem. Res.* **2012**, *46*, 399−411. (e) Schramm, M. P.; Rebek, J., Jr. *Chem.—Eur. J.* **2006**, *12*, 5924−5933.

(11) (a) Eckert, J.-F.; Byrne, D.; Nicoud, J.-F.; Oswald, L.; Nierengarten, J.-F.; Numata, M.; Ikeda, A.; Shinkai, S.; Armaroli, N. *New J. Chem.* **2000**, *24*, 749−758. (b) Huerta, E.; Metselaar, G. A.; Fragoso, A.; Santos, E.; Bo, C.; de Mendoza, J. *Angew. Chem., Int. Ed.* **2007**, *46*, 202−205.

(12) (a) Lenthall, J. T.; Steed, J. W. *Coord. Chem. Rev.* **2007**, *251*, 1747−1760. (b) Frischmann, P. D.; MacLachlan, M. J. *Comments Inorg. Chem.* **2008**, *29*, 26−45. (c) Frischmann, P. D.; MacLachlan, M. J. *Chem. Soc. Rev.* **2013**, *42*, 871−890. (d) Han, Y.-F.; Li, H.; Jin, G.-X. *Chem. Commun.* **2010**, *46*, 6879−6890. (e) Huang, C.-C.; Liu, J.-J.; Chen, Y.; Lin, M.-J. *Chem. Commun.* **2013**, *49*, 11512−11514.

(13) (a) Garon, C. N.; Daigle, M.; Levesque, I.; Dufour, P.; Iden, H.; Tessier, C.; Maris, T.; Morin, J.-F.; Fontaine, F.-G. *Inorg. Chem.* **2012**, *51*, 10384−10393. (b) Garon, C. N.; Gorelsky, S. I.; Sigouin, O.; Woo, T. K.; Fontaine, F.-G. *Inorg. Chem.* **2009**, *48*, 1699−1710. (c) Sigouin, O.; Garon, C. N.; Delaunais, G.; Yin, X.; Woo, T. K.; Decken, A.; Fontaine, F.-G. *Angew. Chem., Int. Ed.* **2007**, *46*, 4979−4982.

(14) (a) Corbett, J. D. *J. Chem. Soc., Dalton Trans.* **1996**, 575−587. (b) Cotton, F. A.; Wilkinson, G.; Murillo, C. A.; Bochmann, M. *Advanced Inorganic Chemistry*, 6th ed.; John Wiley & Sons: New York, 1999; pp 889−892.

(15) Hidalgo, G.; Pellinghelli, M. A.; Royo, P.; Serrano, R.; Tiripicchio, A. *J. Chem. Soc., Chem. Commun.* **1990**, 1118−1120.

(16) Niehues, M.; Erker, G.; Meyer, O.; Fröhlich, R. *Organometallics* **2000**, *19*, 2813−2815.

(17) Zhou, Y.-K.; Chen, H.-M. *Polyhedron* **1990**, *9*, 2689−2691.

(18) Zhang, R.-F.; Li, C.-P.; Wang, Q.-F.; Ma, C.-L. *J. Coord. Chem.* **2010**, *63*, 2105−2112.

(19) Li, J.; Gao, Z.; Han, L.; Gao, L.; Zhang, C.; Tikkanen, W. *J. Organomet. Chem.* **2009**, *694*, 3444−3451.

(20) (a) Feng, X. J.; Tian, P. Z.; Xu, Z.; Chen, S. F.; Wong, M. S. *J. Org. Chem.* **2013**, *78*, 11318−11325. (b) Aoun, O.; Benamara, S.; Aberkane, L.; Amrani, N.; Dahmoune, F.; Madani, K. *Anal. Methods* **2013**, *5*, 5830−5835.

(21) (a) Evans, R. C.; Douglas, P.; Winscom, C. *Coord. Chem. Rev.* **2006**, *250*, 2093−2126. (b) Hudson, Z. M.; Wang, S. *Dalton Trans.* **2011**, *40*, 7805−7816.

(22) Sajoto, T.; Djurovich, P. I.; Tamayo, A. B.; Oxgaard, J.; Goddard, W. A., III; Thompson, M. E. *J. Am. Chem. Soc.* **2009**, *131*, 9813−9822.

(23) (a) Yang, L.; Okuda, F.; Kobayashi, K.; Nozaki, K.; Tanabe, Y.; Ishii, Y.; Haga, M. A. *Inorg. Chem.* **2008**, *47*, 7154−7165. (b) Rausch, A. F.; Murohy, L.; Williams, J. A. G.; Yersin, H. *Inorg. Chem.* **2012**, *51*, 312−319.

(24) Homnick, P. J.; Lahti, P. M. *Phys. Chem. Chem. Phys.* **2012**, *14*, 11961−11968.

(25) *APEX2*; Bruker AXS Inc.: Madison, WI, 2007.

(26) *SAINT*; Bruker AXS Inc.: Madison, WI, 2007.

(27) Sheldrick, G. M. *SADABS*; Bruker AXS Inc.: Madison, WI, 2007.

(28) Sheldrick, G. M. *Acta Crystallogr.* **2008**, *A64*, 112−122.

(29) Spek, A. L. *Acta Crystallogr.* **2009**, *D65*, 148−155.